DMD Fast Forward. Published on January 12, 2007 as doi:10.1124/dmd.106.013581

Identification and Functional Characterization of Genetic Variants of Human Organic Cation Transporters (hOCTs) in a Korean Population

Ho-Jin Kang, Im-Sook Song, Ho Jung Shin, Woo-Young Kim, Choong-Hee Lee, Joo-Cheol Shim, Hong-Hao Zhou, Sang Seop Lee, and Jae-Gook Shin

Department of Pharmacology and PharmacoGenomics Research Center, Inje University College of Medicine, Busan 614-735, Korea (H.J.K., I.S.S., H.J.S., W.Y.K., C.H.L., J.C.S., S.S.L., J.G.S.); and Institute of Clinical Pharmacology, Xiang-Ya School of Medicine, Central South University, Changsha 410078, China (H.H.Z.)

Running title: POLYMORPHISMS OF *hOCTs* IN KOREAN SUBJECTS

Address correspondence to: Jae-Gook Shin, MD, PhD, Department of Pharmacology and PharmacoGenomics Research Center, Inje University College of Medicine,

633-165 Gaegum 2-Dong, Jin-Gu, Busan 614-735, Korea

Tel: +82-51-890-6709; Fax: +82-51-893-1232; E-mail: phshinjg@inje.ac.kr

Number of Text pages: 31 pages

Number of Tables: 3 pages

Number of Figures: 5 figures

Number of References: 28 references

Number of Words in Abstract: 245 words

Number of Words in Introduction: 690 words

Number of Words in Discussion: 1,493 words

ABBREVIATIONS: hOCT, human organic cation transporter; SNP, single nucleotide polymorphism; TEA, tetraethyl ammonium; MPP^+, methyl-4-phenylpyridinium acetate; CL_{int}, intrinsic clearance

DMD Fast Forward. Published on January 12, 2007 as DOI: 10.1124/dmd.106.013581
This article has not been copyedited and formatted. The final version may differ from this version.

ABSTRACT:

Genetic variants of three human organic cation transporter genes (*hOCT*s) were extensively explored in a Korean population, the functional changes of *hOCT2* variants were evaluated *in vitro*, and also compared those genetic polymorphisms of *hOCT*s among different ethnic populations. From direct DNA sequencing, Seven of 13 coding variants were non-synonymous SNPs including four variants from *hOCT1* (F160L, P283L, P341L, and M408V) and three from *hOCT2* (T199I, T201M, and A270S), while six were synonymous SNPs. The linkage disequilibrium analysis presented for three independent LD blocks for each *hOCT* gene showed no significant linkage among all three *hOCT* genes. The transporter activities of MDCK cells that overexpressing the hOCT2-T199I, -T201M, and -A270S variants showed significantly decreased uptake of [^{3}H]MPP^{+} or [^{14}C]TEA compared to those cells that overexpressing wild-type hOCT2, and the estimated kinetic parameters of these variants for [^{3}H]MPP^{+} uptake in oocytes showed a 2-5-fold increase in K_m values and a 10-20-fold decrease in V_{max} values. The allele frequencies of the five functional variants *hOCT1*-P283L, -P341L, and *hOCT2*-T199I, -T201M, and -A270S were 1.3, 17, 0.7, 0.7, and 11%, respectively, in a Korean population; the frequency distributions of these variants were not significantly different to those of Chinese and Vietnamese populations. These findings suggest that genetic variants of *hOCT*s are not linked among 3 genes in a Korean population, and several of the *hOCT* genetic variants cause decreased transport activity *in vitro* compared to the wild type although the clinical relevance of these variants remains to be evaluated.

Introduction

The human organic cation transporters hOCT1, hOCT2, and hOCT3 mediate electrogenic transport of small organic cations with different molecular structures, independent of sodium gradient (Koepsell, 1999). These organic cation substrates include clinically important therapeutics (e.g., metformin, procainamide, and cimetidine), endogenous compounds (e.g., dopamine and norepinephrine), as well as toxic substances (e.g., TEA, HPP^+, and MPP^+) (Kang et al., 2006; Zhang et al., 1997; Gorboulev et al., 1997). Although these transporters show extensive overlaps in their substrate specificities, they exhibit distinct differences in tissue distribution; hOCT1 is primarily found in the sinusoidal membrane of hepatocytes and, to a lesser extent, in intestinal epithelial cells, whereas hOCT2 is mainly expressed in the basolateral membrane of kidney proximal tubules, and hOCT3 shows a widespread tissue distribution, which includes the brain, heart, and liver. Based on their properties and tissue distributions, hOCT1, hOCT2, and hOCT3 are thought to play important roles in the excretion and distribution of organic cations in the liver, kidney, and brain (Jonker and Schinkel, 2004).

Knockout mouse models have been generated for the *Oct1*, *Oct2*, and *Oct3* genes, to elucidate the *in vivo* function of the OCT transporters. Oct1-, Oct2-, and Oct3-deficient mice are viable and display no obvious phenotypic abnormalities (Jonker and Schinkel, 2004; Jonker et al., 2001; Jonker et al., 2003; Wang et al., 2002; Wang et al., 2003; Zwart et al., 2001). However, Oct1 gene knockout mice show dramatically reduced hepatic uptake of TEA and metformin (Jonker et al., 2001; Wang et al., 2002; Wang et al., 2003). In Oct1/2 double-knockout mice, the renal secretion of TEA is completely abolished and the plasma levels of TEA are substantially increased (Jonker et al., 2003). Considering the differences in tissue distribution between mice and humans, a combined deficiency of Oct1 and Oct2 better reflects the effect of OCT2 deficiency on kidney function (Jonker and Schinkel, 2004). The accumulation of MPP^+ in the

heart and fetus is significantly reduced in Oct3-deficient mice compared to wild-type mice (Jonker and Schinkel, 2004; Zwart et al., 2001).

Recently, several groups have reported polymorphic variations in the hOCT families. Twenty-five genetic polymorphisms of *hOCT1* were identified in 57 Caucasians subjects (Kerb et al., 2002) and three (R61C, C88R, and G401S) out of eight non-synonymous variants showed reduced transport activities. Shu et al. (2003) have reported a total of 15 protein-altering variants of *hOCT1* from diverse ethnic backgrounds, and three variants (F160L, P341L, and M408V) were identified in all the ethnic groups. Four SNPs (R61C, G220V, G401S, and G465R) show reduced transport function, whereas S14F exhibits increased transport function. Three non-synonymous SNPs (P283L, R287G and P341L) of *hOCT1* found in a Japanese population show reduced transport activity (Sakata et al., 2004; Takeuchi et al., 2003). Two SNPs (M165I and R400C) out of the eight genetic variants of *hOCT2*, each with an allele frequency of more than 1% in an African-American population, display significantly reduced transport activity (Leabman et al., 2002). The variant (A270S) with the highest allele frequency has a subtle effect on hOCT2 function (Leabman et al., 2002). Fujita et al. (2006) have also reported that A270S has a higher K_i value for tetrabutyl ammonium inhibition of MPP^+ uptake (274 μM) than that of wild-type hOCT2 (148 μM). Several genomic variants, such as R120R and A411A, have been identified in *hOCT3* without amino acid substitution (Lazar et al., 2003).

Since the genetic variants associated with impaired transport function *in vitro* may have an influence on substrate disposition *in vivo* (Kerb et al., 2002; Shu et al., 2003), it is of importance to identify the functional polymorphisms and ethnic diversity of the three *hOCT* genes, in order to understand inter-individual differences in the disposition and distribution of organic cations. However, little information is available regarding genetic polymorphisms of the *hOCT* genes in the Korean population or on the ethnic differences among Asian groups regarding

genetic polymorphisms related to impaired functional activity of hOCT transporters. Therefore, in this study, we evaluated extensively genetic polymorphisms of the three *hOCT* genes in Korean subjects and investigated the functional properties of the non-synonymous SNPs. Moreover, we performed ethnic comparisons of the major functional SNPs of the hOCT transporter genes.

Materials and Methods

Reagents. Methyl-4-phenylpyridinium acetate, N-[methyl-^{3}H], -MPP^{+} (3.21 TBq/mmol) and tetraethylammonium bromide, [1-^{14}C]-, TEA (185 MBq/mmol) were purchased from PerkinElmer (Boston, MA). Cell culture reagents, which included Dulbecco's modified Eagle's medium (DMEM), fetal bovine serum, and trypsin, were purchased from Gibco-BRL (Tokyo, Japan). Lipofectamine 2000 was purchased from Gibco-BRL.

Subjects. Korean subjects (N = 150) were recruited for this *hOCT* genotyping study. Among these 150 subjects, 50 subjects were used to identify SNPs by full DNA sequencing. All of the participants were healthy according to their medical histories, physical examination, and routine laboratory tests. All of the subjects provided written informed consent before participating in the present study, which was approved by the Institutional Review Board of Busan Paik Hospital (Busan, Korea). Genomic DNA samples from 100 Vietnamese and 100 Chinese subjects, which were stored in the DNA repository of PharmacoGenomics Research Center, Inje University (Busan, Korea), were used for the *hOCT* genotyping study. The racial background of the Vietnamese subjects was Viet Kinh, a major population group in Vietnam, and all the Chinese subjects were Han. The 100 DNA samples from German Caucasians were kindly provided by Ulrich M. Zanger of the Dr. Margarete Fischer-Bosch Institute of Clinical Pharmacology (Stuttgart, Germany).

DNA purification and direct sequencing. For direct sequencing of the *hOCT1*, *hOCT2*, and *hOCT3* genes, genomic DNA samples were isolated from the whole blood cells of 150 healthy Korean subjects using the Qiagen DNA Extraction Kit (Qiagen, Valencia, CA) according to the manufacturer's protocol. Specific primers were designed using the Primer3 software

(http://frodo.wi.mit.edu/cgi-bin/primer3/primer3_www.cgi), to amplify 11 exons and the proximal promoter regions of each of the *hOCT1*, *hOCT2*, and *hOCT3* genes (Table 1). PCR was performed in a reaction volume of 25 μl in the presence of 150 ng of genomic DNA, 1× PCR buffer, 0.2 mM dNTPs, 0.2 μM of each primer, and 1 U Taq polymerase (Roche Applied Science, Penzberg, Germany). PCR was performed in the GeneAmp PCR 9700 (Applied Biosystems, Foster City, CA), with an initial denaturation step of 94 °C for 5 min, followed by 30 cycles of denaturation at 95 °C for 1 min, annealing at 54–69 °C for 1 min, and extension at 72 °C for 1 min. A final termination of elongation step was performed at 72 °C for 5 min. The sequences of all the primers and details of the annealing temperatures are listed in Table 1. Amplicons were sequenced using an automated sequencer with the BigDye Terminator Sequencing Kit (Applied Biosystems).

Pyrosequencing analysis. The primers used for pyrosequencing the *hOCT1* and *hOCT2* variants are summarized in Table 1. Biotinylated PCR products were immobilized onto streptavidin-coated beads (Streptavidin Sepharose High Performance; GE Healthcare Biosciences, Piscataway, NJ) following strand separation for use in the PSQ 96 Sample Preparation Kit (Pyrosequencing; GE Healthcare Biosciences). Briefly, the mixture of Sepharose bead slurry (3 μl), binding buffer (37 μl), PCR product (15 μl), and distilled water (25 μl) was incubated at room temperature for 10 min, and then centrifuged at 1,400 rpm. The beads were transferred to a filter plate and the liquid was removed by vacuum filtration (Multiscreen Resist Vacuum Manifold; Millipore Inc., Billerica, MA). The DNA strands were separated in denaturation solution (0.5 M NaOH) for 5 sec. The immobilized template was washed with 10 mM Tris-acetate washing buffer (pH 7.6), transferred to a PSQ 96 plate, and resuspended in 20 mM Tris-acetate annealing buffer (pH 7.6)

that contained the sequencing primer. The sequencing primer was annealed at 80-90 °C for 3 min. The sequence was analyzed using the PSQ 96 system with the SNP Reagent Kit (GE Healthcare Biosciences).

Plasmids. To construct the hOCT2 expression plasmid (pcDNA3.1-hOCT2), we amplified *hOCT2* cDNA (GenBank accession no. NM_003058) by PCR using the primer pair of 5′-GCCGGTACCATGCCCACCACCGTGGAC-3′ and 5′-GCCGGTACCTTAGTTCAATGGAATGTCTAGTTTCTG-3′ (underlined is the recognition site for *Kpn*I) and the template of pEXO-hOCT2 (kind gift from Kathleen M. Giacomini, University of California at San Francisco). The isolated cDNAs were subcloned into the *Kpn*I site of pcDNA3.1(-).

To obtain mutant plasmids of hOCT2-T199I, -T201M, and -A270S, mutagenesis reactions were carried out on the DNA template of pcDNA3.1-hOCT2 using the Quick Change Site-directed Mutagenesis Kit (Stratagene, La Jolla, CA) according to the manufacturer's instructions. The mutations, as well as the fidelity of the remaining DNA, were confirmed by sequencing. The double-stranded oligonucleotides used for site-directed mutagenesis of the *hOCT2* gene were as follows: T199I, forward 5´-GTTCTCATGGCCATTTCCCCAATCTATACGTGGATG-3´ and reverse 5´-CATCCACGTATAGATTGGGGAAATGGCCATGAGAAC-3´; T201M, forward 5´-GGCCATTTCCCCAACCTATATGTGGATGTTAATTTTTCGC-3´ and reverse 5´-GCGAAAAATTAACATCCACATATAGGTTGGGGAAATGGCC-3´; and A270S, forward 5´-GTGGTTGCAGTTCACAGTTTCTCTGCCCAACTTCTTCTTC-3´ and reverse 5´-GAAGAAGAAGTTGGGCAGAGAAACTGTGAACTGCAACCAC-3´

Cellular uptake studies. MDCK cells were maintained in a humidified atmosphere of 5% CO_2 and 95% air and grown in DMEM that was supplemented with 10% fetal bovine serum, 2 mM L-glutamine, and 100 U/ml penicillin-streptomycin. The medium was changed every two days. After the culture had reached 90% confluence, the cells were trypsinized and seeded onto 12-well plates at a density of 3×10^5 cells per well. At 80% confluence, the cell culture medium was substituted with serum-free medium, 2 hr before transfection. Transient transfections of pcDNA3.1 and pcDNA3.1-hOCT2 wild-type and mutants were performed into MDCK cells using Lipofectamine 2000. After transfection, the cells were incubated for 48 hr at 37 °C. Uptake studies were performed after the transfected cells formed a monolayer. The medium was removed from the MDCK cell cultures, the cells were washed with Eagle's medium, and pre-incubated for 1 hr with serum-free DMEM at 37 °C. The uptake was initiated by replacing the medium with 1 ml of serum-free DMEM that contained 200 nM [^{3}H]MPP$^+$ or [^{14}C]TEA, and quenched by washing three times with 2 ml of ice-cold PBS. The cells were lysed with 100 µl of cell lysis reagent (CCLR buffer; Promega, Madison, WI) that was composed of 100 mM potassium phosphate (pH 7.8), 1 mM EDTA, 7 mM 2-mercaptoethanol, 1% (v/v) Triton X-100, and 10% (v/v) glycerol. The radioactivity of the cell lysates was measured by a MicroBeta TriLux 96-well Scintillation/Luminescence detector (PerkinElmer).

Western Blotting. The transfected MDCK cells were harvested by centrifugation at 6,000 rpm for 3 min at 4°C in an Eppendorf 5415R centrifuge. Cell pellets were swelled in one volume of RIPA cell lysis buffer [150 mM NaCl, 1% NP-40, 0.5% sodium deoxycholate, 0.1% SDS, 50 mM Tris (pH 7.5)] for 10 min. Aliquots that contained 30 µg of protein were separated by SDS-PAGE in a 4-12% gradient gel (Invitrogen, Carlsbad, CA) and transferred to nitrocellulose membranes (Bio-Rad, Hercules, CA). The membranes were blocked with 5% nonfat milk and

probed with anti-OCT2 (Santa Cruz Biotechnology, Santa Cruz, CA), and anti-actin antibodies (Cell Signaling Technology, Beverly, MA). The membranes were then incubated with horseradish peroxidase-conjugated anti-goat IgG or anti-rabbit IgG (Santa Cruz Biotechnology) and visualized using the ECL system (Santa Cruz Biotechnology).

cRNA synthesis and transport measurements using *X. Laevis* oocytes. The cRNA synthesis and uptake experiments were performed as described previously (Kusuhara et. al., 1999). The capped cRNAs were synthesized *in vitro* using T7 RNA polymerase with linear plasmid DNA. Defolliculated oocytes were injected with 50 ng of the capped cRNA and incubated at 18 °C in Barth's solution [88 mM NaCl, 1 mM KCl, 0.33 mM $Ca(NO_3)_2$, 0.4 mM $CaCl_2$, 0.8 mM $MgSO_2$, 2.4 mM $NaHCO_3$, 10 mM Hepes (pH 7.4)] that contained 50 μg/ml gentamicin and 2.5 mM pyruvate. After incubation for 2 days, uptake experiments were performed at room temperature in ND96 solution [96 mM NaCl, 2 mM KCl, 1.8 mM $CaCl_2$, 1 mM $MgCl_2$, 5 mM Hepes, (pH 7.4)]. The uptake reaction was initiated by replacing the ND96 solution with one that contained the radiolabeled ligand, and terminated by the addition of ice-cold ND96 solution. After washing five times, oocytes were solubilized with 10% SDS and the radioactivity in the oocytes was analyzed.

Immunofluorescence analysis. *X. laevis* oocytes were injected with the cRNAs for the hOCT2 wild-type and mutants. Two days after injection, the oocytes were fixed with paraformaldehyde and incubated with the anti-hOCT2 antibody (Santa Cruz Biotechnology; dilution 1:50), followed by FITC-labeled rabbit anti-goat IgG (Santa Cruz Biotechnology; dilution 1:200). The sections were examined under a Carl Zeiss LSM 510 META confocal microscope (Carl Zeiss Inc., Jena, Germany).

Linkage disequilibrium analysis. The population genetic analysis program Haploview version 3.2 was used for the linkage disequilibrium (LD) analysis and Hardy-Weinberg equilibrium (HWE) test. The Haploview software calculates marker metrics and allows the visualization of haplotype block structures (Gabriel et al., 2002; Barrerr et al., 2005). Initially, we genotyped the SNPs of the *hOCT1*, *hOCT2*, and *hOCT3* genes, and subsequently embedded them into the LD blocks for Korean subjects. The pairwise LD between all the SNP pairs was estimated by calculating the |D′| values using the haplotype blocks described by Gabriel et al. (2005). All the genotyped results were checked to make sure that they did not deviate from HWE by the *p*-value cutoff at 0.05. To rule out genotyping errors and recently accrued *hOCT1*, *hOCT2*, and *hOCT3* mutations, a minor allele frequency (MAF) of at least 10% was used. The allele frequencies, individual genotypes, and assays can be downloaded in bulk from our website, and can also be browsed graphically.

For pairwise comparisons of allele frequencies between different ethnic groups, the χ^2 test was performed using the SAS program (SAS Institute, Cary, NC), and $p < 0.05$ was considered to be statistically significant.

Data analysis. Cellular uptake was calculated as the cell/medium ratio based on the intracellular uptake per microgram of cell protein (dpm/μg protein) relative to the initial drug concentration. Statistical significance was analyzed using the unpaired *t*-test, and $p < 0.05$ was considered to be statistically significant. The reproducibility of the results in the present study was confirmed using three separate experiments. The data are expressed as the mean ± S.D.

To estimate the kinetic parameters for the uptake of [^{3}H]MPP$^+$ by X. *Laevis* oocytes

DMD Fast Forward. Published on January 12, 2007 as DOI: 10.1124/dmd.106.013581
This article has not been copyedited and formatted. The final version may differ from this version.

overexpressing hOCT2 wild-type and variants, the hOCT2-mediated uptake rates were calculated by subtracting the transport rate of noninjected oocytes from that of hOCT2-expressing oocytes, followed by fitting to the Michaelis-Menten curve by an iterative nonlinear least squares method using the WinNonlin version 5.1 (Pharsight, Mountain View, CA). Intrinsic clearance (CL_{int}) was obtained by dividing V_{max} values by K_m values.

Results

Identification of genetic variations of the *hOCT* genes in Korean subjects. To identify genetic polymorphisms of *hOCT1, hOCT2,* and *hOCT3,* we screened all 11 exons and approximately 2 kb of the 5′-flanking sequence of each transporter gene, as well as 50-100 bp of the flanking intronic sequences. The genetic variants and their frequencies for the *hOCT1, hOCT2,* and *hOCT3* genes in 50 Korean subjects are summarized in Table 2. Sixteen variants were identified in the non-coding or intronic regions and thirteen were identified in coding regions. Six SNPs of the coding region were synonymous and seven were non-synonymous. Among 7 non-synonymous SNPs, hOCT1-F160L and hOCT1-M408V did not cause functional changes and hOCT1-P283L, hOCT1-P341L, and hOCT2-A270S were reported to show decreased transport activity. Fourteen novel SNPs including 11 SNPs in the 5'-UTR region, 2 SNPs in the non-coding region, and 1 SNP in the coding region were identified.

To reveal the genetic structures of the *hOCT1, hOCT2,* and *hOCT3* loci in this Korean population, pairwise LD was analyzed using common variants of *hOCT1, hOCT2,* and *hOCT3.* All of the SNPs were in Hardy-Weinberg equilibrium (HWE, $p > 0.05$). The *hOCT1, hOCT2,* and *hOCT3* genes are all located on chromosome 6q26-27 and were non-uniformly distributed across the 333-kb contiguous sequence (Fig. 1). In order to evaluate the impact of *hOCT1, hOCT2,* and *hOCT3* variants on the block structure, we analyzed the values of $|D'|$ and r^2 between 16 variant sites [minor allele frequencies (MAF) >10%, $p < 0.05$]. As shown in the LD block analysis (Fig. 1), there appear to be only three major haplotype blocks for each of the *hOCT1, hOCT2,* and *hOCT3* loci: the first block spans the E5+45G>A and 1022A>G SNPs (*hOCT1*); the second block spans the 808G>T and E2+32C>G SNPs (*hOCT2*); and the third block spans from the -2269C>T SNP to the 360T>C SNP (*hOCT3*). LD analysis for hOCT variants with more than 10% frequency in Korean subjects showed no significant linkage between the *hOCT* genes, which

suggests that the mutations in these three transporters are independent.

Functional analysis of hOCT2 variants *in vitro*. The non-synonymous SNPs, which included P283L and P341L of the *hOCT1* gene, have been reported to show reduced transport activities (Sakata et al., 2004; Takeuchi et al., 2003), whereas little is known about the functional activities of the non-synonymous SNPs of hOCT2 (T199I and T201M) (Fukushima-Uesaka et al., 2004). To evaluate the transport activity of genetic variants of hOCT2, the expression vectors containing hOCT2-WT, -T199I, -T201M, and -A270S were transiently transfected into MDCK cells. The uptake of [^{3}H]MPP$^+$ and [^{14}C]TEA was increased linearly up to 15 min and 30min, respectively (Data not shown). As shown in Fig. 2, the uptake rates of [^{3}H]MPP$^+$ and [^{14}C]TEA were significantly lower for the T199I, T201M, and A270S SNPs than for the wild-type hOCT2. However, the protein expression levels of the hOCT2 wild-type and variants were not changed in transiently transfected MDCK cells (Fig. 2C).

To determine the kinetics of uptake of [^{3}H]MPP$^+$ *via* the hOCT2 wild-type and SNP variants (T199I, T201M, and A270S) expressed in *X. Laevis* oocytes, the concentration dependency of the uptake rates of [^{3}H]MPP$^+$ was studied within the range of 0.005–30 μM (Fig. 3). The uptake of [^{3}H]MPP$^+$ was increased linearly up to 60 min (data not shown) and the uptake rate of [^{3}H]MPP$^+$ showed concentration dependency with increased concentration of MPP$^+$ (Fig. 3A). Kinetic parameters such as K_m, V_{max}, and intrinsic clearance (CL_{int}) were shown in Fig. 3B. The approximate V_{max} values for the hOCT2-T199I, -T201M, and -A270S SNPs were 22.5, 21.7, 11.7-fold decreased, respectively, compared with that for hOCT2-WT; The approximate K_m values for the hOCT2-T199I, -T201M, and -A270S SNPs were 3.7, 5.1, 2.0-fold increased, respectively, compared with that for hOCT2-WT; and the approximate CL_{int} (obtained by dividing V_{max} by K_m) for the hOCT2-T199I, -T201M, and -A270S SNPs were 83.7, 110.4, 23.4-

fold decreased, respectively, compared with that for hOCT2-WT. The localizations of the hOCT2 wild-type and variant proteins in *X. laevis* oocytes were revealed by immunofluorescence analysis. No expression was shown when empty vector was injected into oocytes (Fig. 4A). The hOCT2 wild-type protein (Fig. 4B) and variant proteins (Fig. 4C, D, and E) were highly expressed and localized in the plasma membrane.

Ethnic frequencies of functional variants of hOCTs. The occurrence of functional variants of hOCT1 (P283L and P341L) and hOCT2 (T199I, T201M and A270S) was analyzed by pyrosequencing analysis of 150 Korean subjects and 100 subjects each of Vietnamese, Chinese, and German Caucasian origin. The pyrosequencing-based genotypes of 450 DNA samples were completely concordant with the data obtained by the reference method of direct sequencing, which suggests that the simplex and duplex assay methods developed in this study are time efficient and can be applied to the genotyping of five functional SNPs of the *hOCT* genes (Fig. 5).

Genotyping results and allele frequencies of the hOCT1-P283L, hOCT1-P341L, hOCT2-T199I, hOCT2-T201M, and hOCT2-A270S variants from different ethnic groups were shown in Table 3. Six subjects were homozygous for hOCT1-P341L (one in Korean and one in Chinese group) and *hOCT2*-A270S (one in Korean and three in Chinese group), and the remaining variants were heterozygous (Table 3). The observed distributions for all the alleles were in accordance with the distributions predicted by the Hardy-Weinberg law. The allele frequencies of hOCT1-P341L and hOCT2-A270S in Korean subjects were very close to those observed in other Asian populations (5.5-17% and 11-14%, respectively) but different significantly from those observed in German Caucasians (2% and 2.5%, respectively). The remaining three functional variants (hOCT1-P283L, hOCT1-T199I, and hOCT2-T201M) were rare SNPs with frequencies <1%, and they showed no differences in distribution among the different ethnic groups.

DMD Fast Forward. Published on January 12, 2007 as DOI: 10.1124/dmd.106.013581
This article has not been copyedited and formatted. The final version may differ from this version.

Discussion

To understand the potential effects of genetic variations on xenobiotic transport activity, we carried out a comprehensive genetic polymorphism analysis of the human organic cation transporters hOCT1, hOCT2, and hOCT3. Twenty nine genetic mutations of *hOCT1, hOCT2,* and *hOCT3* were recognized in the Korean subjects, and seven non-synonymous variants, hOCT1-F160L, -P283L, -P341L, and -M408V and hOCT2-T199I, -T201M, and -A270S, were identified. Among them, the functional consequences of non-synonymous SNPs of hOCT1 were well defined (Table 2), whereas little is known about the functional activities of those of hOCT2 (T199I and T201M). Thus, we evaluated the functional activities of the non-synonymous SNPs of hOCT2 using MDCK cells and *X. laevis* oocytes. MDCK cells that overexpressing hOCT2-T199I, -T201M, and -A270S showed decreased uptake of [^{3}H]MPP^{+} and [^{14}C]TEA compared to the wild-type (Fig. 2). MDCK cells are originated from canine kidney epithelium and express endogenous OCT2 transporter (Shu et al., 2001), which was consistent with the western results that showed basal expression in empty vector transfected MDCK cells (Fig. 2C). This may be reasons that uptake rates of [^{3}H]MPP^{+} and [^{14}C]TEA in empty vector transfected MDCK cells were 36% and 44% of those in wild type hOCT2 transfected cells, respectively. If the uptake rates of [^{3}H]MPP^{+} and [^{14}C]TEA mediated by endogenous OCT2 were subtracted from those of transfected hOCT2-WT and variants, the uptake rates of [^{3}H]MPP^{+} in hOCT2 variants (T199I, T201M, and A270S) were decreased to 38%, 46%, and 59% of hOCT2-WT, respectively, and the uptake rates of [^{14}C]TEA in hOCT2 variants were decreased to 36%, 24%, and 41% of hOCT2-WT, respectively. To rule out the involvement of endogenous OCT2 in kinetic parameters of hOCT2 WT and variants, we measured concentration dependent uptake of [^{3}H]MPP^{+} in *X. Laevis* oocytes which show no endogenous OCT2 expression. Kinetic analysis of the hOCT2 mutants confirmed the functional changes of these variants, as evidenced by increased values of

approximate K_m, and decreased values of approximate V_{max} and CL_{int} of all three hOCT2 variants compared to the wild-type hOCT2. There has been some controversy regarding the functional activity of the A270S variant due to the slight (approximately 2-fold) change in the K_i value of this mutant (Leabman et al., 2002; Fujita et al., 2006), which is consistent with our results. However, transport function should be evaluated in terms of CL_{int}, as well as K_m and V_{max}. According to our results, the approximate CL_{int} of the A270S variant was decreased 23.4-fold, which suggests decreased transport activity for the A270S mutant. However, the protein expression level and localization of the hOCT2 variants in MDCK cells and *X. laevis* oocytes were not different from those of the wild-type (Figs. 2 and 4). These results, taken together, suggest that the reduced transport activities of the hOCT2 variants (T199I, T201M, and A270S) are not attributable to either protein expression or plasma membrane localization.

The five functional variants of hOCT1 and hOCT2 are distributed throughout the loops (hOCT1-P283L and -P341L and hOCT2-T199I and -T201M) and transmembrane domains (hOCT2-A270S) of the protein, according to the presumed transmembrane topology of hOCT transporters (Leabman et al., 2002; Popp et al., 2005). Considering that several cysteine, proline, and arginine residues are thought to maintain the secondary structures of proteins and/or bind charged substrates (Burckhardt et al., 2000), the reduced functional activities of hOCT1 (Sakata et al., 2004; Takeuchi et al., 2003) and hOCT2 caused by amino acid substitutions may be related to structural changes in the substrate recognition region and/or functional domain. The changes in approximate V_{max} values (11.7–22.5-fold change) of the hOCT2-T199I, -T201M, and -A270S mutants in the third extracellular loop and sixth transmembrane domain of the hOCT2 transporter were larger than the changes in the approximate K_m values (2.0–5.1-fold change) of the variants. The critical amino acids of Tyr222 and Thr226 in the substrate-binding pocket of hOCT1 are highly conserved among the hOCT subtypes of various species and are located in the fourth

transmembrane domain (Popp et al., 2005). Therefore, the amino acid substitutions in hOCT2-T199I, -T201M, and -A270S mutants might have inhibitory effects on conformational changes of the transporter rather than on substrate binding.

The allele frequencies of the hOCT1 (P283L and P341L) and hOCT2 (T199I, T201M, and A270S) variants were analyzed in Korean, Vietnamese, Chinese, and German Caucasian subjects by pyrosequencing. The hOCT1-P283L, hOCT2-T199I, and hOCT2-T201M SNPs were detected very rarely, and showed no differences between Asians and German Caucasians, which indicates that it is not useful to genotype routinely these mutations for predictions of in vivo distribution and disposition of organic cations. On the other hand, the allele frequencies of hOCT1-P341L and hOCT2-A270S in the Korean population (17% and 11%, respectively) were similar to those in other Asian populations, and significantly higher than those in the German Caucasian population (2% and 2.5%, respectively). Therefore, impaired transport activities related to hOCT1-P341L and hOCT2-A270S SNPs may differ between Asians and German Caucasians, with consequent effects on the pharmacokinetics of certain substrates. The *hOCT1*-P341L variant was identified in a German Caucasian population in this study, whereas this mutation was not reported in a Caucasian and European-American population (Kerb et al., 2002; Shu et al., 2003). In addition, the *hOCT2*-A270S mutation revealed different allele frequencies between the Caucasian and German Caucasian populations [i.e., 15.7% for Caucasians (Leabman et al., 2002) and 2.5% for our population]. The lower diversity of the German Caucasian population compared to the European-American and Caucasian pool may explain the different frequencies observed for hOCT1-P341L and hOCT2-A270S.

On the contrary to those non-synonymous SNPs of *hOCT1* and *hOCT2* genes, only three synonymous variants (R120R, G193G, and A411A) were detected from *hOCT3* gene. The absence of a non-synonymous mutation in the *hOCT3* gene and the positive value of Tajima's D

may reflect selective mechanisms against certain amino acid changes that have operated during the evolution of the human species, and may also be due to demographic factors, such as population subdivision (Lazar et al., 2003). In addition, 13 out of 29 *hOCT* SNPs were detected in the 5'-UTR regions of the individual transporter genes, and several SNPs showed relatively high frequency (> 30%), which raises the possibility that the SNPs in the 5´-UTR regions may affect the regulation of expression of these transporters. Recently, it has been reported that hOCT1 gene is transactivated by Hepatocyte Nuclear Factor-4α (HNF-4α) and that the mRNA expression of organic cation transporters in liver, kidney, and duodenum is altered differently after targeted disruption of the transcription factor HNF-1α (Saborowski et al., 2006; Maher e tal., 2006). Site directed mutagenesis of HNF-4α binding site in the promoter region of hOCT1 gene more strongly decreased luciferase activity of reporter construct hOCT1(-2620/+116)mut than that of wild type reporter construct (Saborowski et al., 2006). Moreover, Shu et al. (2001) reported steroid hormone-mediated regulation of OCT2 in MDCK cells. These reports, taken together, suggested that transcription factors such as HNF-4α and nuclear receptors may be involved in the tissue specific regulation of organic cation transporters. In silico analysis using the TRANSFAC data base (http://www.cbil.upenn.edu/cgi-bin/tess) revealed that several SNPs in 5'-UTR region occurred in the binding sequence for transcription factors such as GATA, Sp1, MyoD, YY1, and c-Myc and the binding sequences for nuclear receptors such as GR, RXR-α, and RAR-α, which suggest that the SNPs in the 5'-UTR region may cause expressional changes of respective transporters. The functional consequences of 13 SNPs in the upstream regions as well as transcriptional regulation of hOCT transporters are under our investigation.

With the identification of functionally important genetic polymorphisms of the *hOCT1* and *hOCT2* genes, it will be of great interest to determine whether these polymorphisms also

correlate with altered drug responses and sensitivities in patients (Jonker and Schinkel, 2004). According to previous reports (Leabman and Giacomini, 2003; Yin et al., 2006), the genetic component that contributes to variation in the renal clearance of metformin, which is a substrate of hOCT2 that is eliminated exclusively by transporter-mediated renal secretion (Fujita et al., 2006; Kimura et al., 2005), is estimated to be particularly high (93%). These findings suggest that variation in the renal clearance of metformin has a strong genetic component, and that genetic variations in hOCT2 may explain, to a large degree, this pharmacokinetic variability (Leabman and Giacomini, 2003). Further studies in humans are underway in our laboratory. In addition, the pyridinium metabolites (HPP^+ and $RHPP^+$) of haloperidol are known to distribute into the brain and cause side-effects, such as neurodegeneration. HPP^+ and $RHPP^+$ are substrates for the hOCT family (Kang et al., 2006). In other words, the uptake of HPP^+ is mediated by hOCT1, hOCT2, and hOCT3, whereas the uptake of $RHPP^+$ is increased in hOCT1- and hOCT3- but not hOCT2-overexpressing MDCK cells. This suggests that functional genetic variants of the hOCT transporters may produce different brain distributions of HPP^+ and $RHPP^+$ and, consequently, different levels of neurotoxicity. Therefore, the information gained about the functional genetic polymorphisms and the ethnic diversity of the hOCT family will help us to understand inter-individual drug responses and the pharmacokinetics of cationic drugs.

Acknowledgments

The hOCT-containing plasmids were kindly provided by Dr. Kathleen M. Giacomini (University of California at San Francisco, CA, USA) and Dr. Hitoshi Endou (Fuji Biomedix Co., Tokyo, Japan).

Reference

Barrerr JC, Fry B, Maller J, and Daly MJ (2005) Haploview: analysis and visualization of LD and haplotype maps. *Bioinformatics* **15**: 263-265.

Burckhardt G and Wolff NA (2000) Structure of renal organic anion and cation transporters. *Am J Physiol Renal Physiol* **278**: F853-F866.

Fujita T, Urban TJ, Leabman MK, Fujita K, and Giacomini KM (2006) Transport of drugs in the kidney by the human organic cation transporter, OCT2 and its genetic variants. *J Pharm Sci* **95**: 25-36.

Fukushima-Uesaka H, Maekawa K, Ozawa S, Komamura K, Ueno K, Shibakawa M, Kamakura S, Kitakaze M, Tomoike H, Saito Y, and Sawada J (2004) Fourteen novel single nucleotide polymorphisms in the SLC22A2 gene encoding human organic cation transporter (OCT2). *Drug Metab Pharmacokinet* **19**: 239-244.

Gabriel SB, Schaffner SF, Nguyen H, Moore JM, Roy J, Blumenstiel B, Higgins J, DeFelice M, Lochner A, Faggart M, Liu-Cordero SN, Rotimi C, Adeyemo A, Cooper R, Ward R, Lander ES, Daly MJ, and Altshuler D (2002) The structure of haplotype blocks in the human genome. *Science* **296**: 2225-2229.

Gorboulev V, Ulzheimer JC, Akhoundova A, Ulzheimer-Teuber I, Karbach U, Quester S, Baumann C, Land F, Busch AE, and Koepsell H (1997) Cloning and characterization of two human polyspecific organic cation transporters. *DNA Cell Biol* **16**: 871-881.

Jonker JW and Schinkel AH (2004) Pharmacological and physiological functions of the polyspecific organic cation transporters: OCT1, 2, and 3 (SLC22A1-3). *J Pharmacol Exp Ther* **308:** 2-9.

Jonker JW, Wagenaar E, Mol CA, Buitelaar M, Koepsell H, Smit JW, and Schinkel AH (2001) Reduced hepatic uptake and intestinal excretion of organic cations in mice with a targeted

disruption of the organic cation transporter1 (Oct1 [Slc22a1]) gene. *Mol Cell Biol* **21:** 5471-5477.

Jonker JW, Wagenaar E, Van Eiji S, and Schinkel AH (2003) Deficiency in the organic cation transporters 1 and 2 (Oct1 and Oct2 [Slc22a1 and Slc22a2]) in mice abolishes the renal secretion of organic cations. *Mol Cell Biol* **23:** 7902-7908.

Kang HJ, Lee SS, Lee CH, Shim JC, Shin HJ, Liu KH, Yoo MA, and Shin JG (2006) Neurotoxic pyridinium metabolites of haloperidol are substrates of human organic cation transporters. *Drug Metab Dispos* **34:** 1145-1151.

Kerb R, Brinkmann U, Chatskaia N, Gorbunov D, Gorboulev V, Mornhinweg E, Keil A, Eichelbaum M, and Koepsell H (2002) Identification of genetic variations of the human organic cation transporter hOCT1 and their functional consequences. *Phamacogenetics* **12**: 591-595.

Kimura N, Masuda S, Tanihara Y, Ueo H, Okuda M, Katsura T, and Inui K (2005) Metformin is a superior substrate for renal organic cation transporter OCT2 rather than hepatic OCT1. *Drug Metab Pharmacokinet* 2005; **20:** 379-386.

Koepsell H (1999) Organic cation transporters in intestine, kidney, liver, and brain. *Annu Rev Physiol* **60**: 243-266.

Lazar A, Grundemann D, Berkels R, Taubert D, Zimmermann T, and Schomig E (2003) Genetic variability of the extraneuronal monoamine transporter EMT (SLC22A3). *J Hum Genet* **48**: 226-230.

Leabman MK and Giacomini KM (2003) Estimating the contribution of genes and environment to variation in renal drug clearance. *Phamacogenetics* **13**: 581-584.

Leabman MK, Huang CC, Kawamoto M, Johns SJ, Stryke D, Ferrin TE, De Young J, Taylor T, Clark AG, Herskowitz I, and Giacomini KM (2002) Pharmacogenetics of Membrane

Transporters investigators: Polymorphisms in a human kidney xenobiotic transporter, OCT2, exhibit altered function. *Pharmacogenetics* **12**:395-405.

Maher JM, Slitt AL, Callaghan TN, Cheng X, Cheng C, Gonzalez FJ, and Klaassen CD (2006) Alterations in transporter expression in liver, kidney, and duodenum after targeted disruption of the transcription factor HNF1a. *Biochem Pharmacol* **72:** 512-522.

Popp C, Gorboulev V, Müller TD, Gorbunov D, Shatskaya N, and Koepsell H (2005) Amino acids critical for substrate affinity of rat organic cation transporter 1 line the substrate binding region in a model derived from the tertiary structure of lactose permease. *Mol Pharmacol* **67**: 1600-1611.

Saborowski M, Kullak-Ublick GA, and Eloranta JJ (2006) The human organic cation transporter-1 gene is transactivated by hepatocyte nuclear factor-4α. *J Pharmacol Exp Ther* **317:** 778-785.

Sakata T, Anzai N, Shin HJ, Noshiro R, Hirata T, Yokoyama H, Kanai Y, and Endou H (2004) Novel single nucleotide polymorphisms of organic cation transporter 1 (SLC22A1) affecting transport functions. *Biochem Biophys Res Commun* **16**: 789-793.

Shu Y, Bello CL, Mangravite LM, Feng B, and Giacomini KM (2001) Functional characterization and steroid hormone-mediated regulation of an organic cation transporter in Madin-Darby Canine Kidney cells. *J Pharmacol Exp Ther* **299:** 392-398.

Shu Y, Leabman MK, Feng B, Mangrabite LM, Huang CC, Stryke D, Kawamoto M, Johns SJ, De Young J, Carlson E, Ferrin TE, Herakowitz I, and Giacomini KM (2003) Evolutionary conservation predicts function of variants of the human organic cation transporter, OCT1. *Proc Natl Acad Sci USA* **100**: 5902-5907.

Takeuchi A, Motohashi H, Okuda M, and Inui K (2003) Decreased function of genetic variants, Pro283Leu and Arg287Gly, in human organic cation transporter hOCT1. *Drug Metab Pharmacokinet* **18**: 409-412.

Wang DS, Jonker JW, Kato Y, Kusuhara H, Schinkel AH, and Sugiyama Y (2002) Involvement of organic cation transporter 1 in hepatic and intestinal distribution of metformin. *J Pharmacol Exp Ther* **302:** 510-515.

Wang DS, Kusuhara H, Kato Y, Jonker JW, Schinkel AH, and Sugiyama Y (2003) Involvement of organic cation transporter 1 in lactic acidosis caused by metformin. *Mol Pharmacol* **63:** 844-848.

Yin OO, Tomlinson B, and Chow MS (2006) Variability in renal clearance of substrates for renal transporters in Chinese subjects. *J Clin Pharmcol* **46:** 157-163.

Zhang L, Dresser MJ, Gray AT, Yost SC, Terashita S, and Giacomini KM (1997) Cloning and functional expression of a human liver organic cation transporter. *Mol Pharmacol* **51:** 913-921.

Zwart R, Verhaagh S, Buitelaar M, Popp-Snijders C, and Barlow DP (2001) Impaired activity of the extraneuronal monoamine transporter system known as uptake-2 in Orct3/Slc22a3-deficient mice. *Mol Cell Biol* **21:** 4188-4196.

Foot note

1. This study was supported by the Korea Science and Engineering Foundation (KOSEF) through the National Research Lab. Program funded by the Ministry of Science and Technology (M10300000370-06J0000-37010) and by a grant of the Korea Health 21 R & D Project, Ministry of Health & Welfare, R. O. K (A030001).

DMD Fast Forward. Published on January 12, 2007 as DOI: 10.1124/dmd.106.013581
This article has not been copyedited and formatted. The final version may differ from this version.

Legends for figures

Fig. 1. Pairwise linkage disequilibrium (LD) among 16 SNPs of the *hOCT1, hOCT2,* and *hOCT3* genes in a Korean population. The cut off p-value of the Hardy-Weinberg equilibrium (HWE) is 0.05. The minimum minor allele frequency (MAF) is 10%.

Fig. 2. Functional characterization of non-synonymous variants of hOCT2 in MDCK cells. MDCK cells were transiently transfected with 1.6 μg of pcDNA3.1-hOCT2, pcDNA3.1-hOCT2-T199I, -T201M, and -A270S. **A and B.** Uptake of [^{3}H]MPP^{+} or [^{14}C]TEA by MDCK cells with over-expressed hOCT2 wild-type or variants. The cells were incubated for 5 min at 37°C after the addition of 200 nM [^{3}H]MPP^{+} or [^{14}C]TEA to the apical side. The uptake of [^{3}H]MPP^{+} or [^{14}C]TEA was determined by measuring radioactivity. Transient transfection of vector, hOCT2-WT, -T199I, -T201M, and -A270S into MDCK cells and uptake study using [^{3}H]MPP^{+} and [^{14}C]TEA were performed three times independently. Bars represent means ± SD. **: $p < 0.01$, relative to the wild-type (WT) and according to the Student's *t*-test. **C.** Western blot analysis was performed using the cell lysates after transient transfection of vector, hOCT2-WT, -T199I, -T201M, and -A270S into MDCK cells. The hOCT2 proteins have molecular sizes in the 50~75-kDa range and were indicated by an arrow.

Fig. 3. Kinetic analysis of the hOCT2 variants. (A) Concentration dependency of [^{3}H]MPP^{+} uptake by oocytes expressing the hOCT2 wild-type and variants (T199I, T201M, and A270S). The uptake of [^{3}H]MPP^{+} was measured at the concentration indicated after 30 min of incubation. Each data point represents the means ± SE after the 8 independent experiments. The level of hOCT2-mediated transport was obtained by subtracting the transport rates of the non-injected oocytes from those of the hOCT2-expressing oocytes. (B) Kinetic parameters were obtained as

approximations by fitting to the Michaelis-Menten curve by an iterative nonlinear least squares method.

Fig. 4. Localization of hOCT2 wild-type and its variants at the plasma membrane of *X. laevis* oocytes. No positive staining for hOCT2 is observed in the control oocytes injected with water instead of cRNAs (**A**). Immunofluorescence detection with hOCT2 antibody shows that the wild-type protein (**B**), as well as the three mutant proteins [T199I (**C**), T201M (**D**), and A270S (**E**)], are expressed at the plasma membrane.

Fig. 5. Genotyping of the functional SNPs of *hOCT1* and *hOCT2* by pyrosequencing. Duplex and simplex assay designs with the expected and observed pyrograms for the hOCT1 (P283L and P341L) and hOCT2 (T199I, T201M, and A270S) variants are shown. The choice of sequence to analyze was based on the cDNA position with attached sequencing primer, which determines the nucleotide dispensation order. For each genotype, a pyrogram is shown, together with a graph of the expected results. Representative pyrograms illustrate heterozygous individuals. The simplex pyrograms show the following genotypes: (**A**) *hOCT1*-P283L (848C/T); (**B**) *hOCT1*-P341L (1022A/G); and (**C**) *hOCT2*-A270S (808G/T). The duplex pyrograms denote the following genotypes: (**D**) *hOCT2*-T199I and -T201M [596C/T (**a**) and 602C/T (**b**)]. The box indicates the position of each SNP.

DMD Fast Forward. Published on January 12, 2007 as DOI: 10.1124/dmd.106.013581
This article has not been copyedited and formatted. The final version may differ from this version.

TABLE 1. Sequences of primers used for amplification of the *hOCT1*, *hOCT2*, and *hOCT3* genes, and the annealing temperatures for PCR

Genes	Positions	Forward Primers (5' to 3')	Reverse Primers (5' to 3')	Annealing (°C)	Products (bp)
For full Sequencing primers					
hOCT1	5'-UTR	TACCTGTCCCCTCAAAACCTATG	GCTCCAGAATGTCATCCACG	57	528
	5'-UTR	TGCAAAGCAGGAAAGTTGAAC	GGGTGACAGCCAGGTACTAGATAC	55	536
	5'-UTR	CCATCCAATCTTAATCAGTTTGATC	TTAAGGTCATAAACTGCTTTGGC	61	581
	5'-UTR	CTAACTTTTAACCATCGCACTCC	AATGGAATACAAGCACAACAAGG	61	548
	5'-UTR	GAAGACTATAATCCATCCCTTGAAG	CTATATTCTCTGCCCCTCCATG	56	608
	Exon 1	TGAGGGAGACATTGCACCTG	GGAACTGAACTTCATAGGATTGC	61	559
	Exon 2	AGTCCTGACTCACACATGGTTC	TGAGAACAGATTCGCCCTTAG	59	240
	Exon 3	CATCCCACCATGCATGTCTG	CCCCTACCCACGTTAGGC	55	293
	Exon 4	AGCTTCTGAACGCACGGC	CGAGAGGACAGAAAGCGCAG	59	315
	Exon 5, 6	GGCTGAACGTCAGACCGAG	AATCTATAGCCCAGTGCTTGG	57	553
	Exon 7	TTTCTTCAGTCTCTGACTCATGC	TCCCCACACTTCGATTGC	57	322
	Exon 8	CAGTAACTCAGGGAACGAAGC	TGAGCTGGTGGGTTCACAG	61	225
	Exon 9	TGAACATTTGGAAAAGTGAATCAC	CAGTTCCACCCATGCTGAG	55	245
	Exon 10	TATTTCTGTAAATGACATTGGCTG	CTTTTGGAGGGCGTGTCAG	57	221
	Exon 11	GACACTTATTCATTTCTGTGTACAAC	ATACAGAGAAGTGAAGGCGTCTAG	57	261
hOCT2	5'-UTR	GGAGAATGAGCCCAGCAGTC	CGAAGGTAGCCGAGAGCAG	69	664
	5'-UTR	ACTGTTACACAGAAAGGCAGCG	GCCCTATGGAGAAAACACACG	60	615
	5'-UTR	TTTTAGACTACGCTATTACACCTGC	ATCCTTCTTCCTCAAAGCAGC	67	690
	5'-UTR	TAAGTGAGTCAAACCCAAGTGC	TCCTGGTGGACAAAGGATC	60	587
	Exon 1	GCAGAAGGACATGCACCC	CCTTGAGAAAATCTCCACCATT	62	677
	Exon 2	TTATGTCCAACAGGATTCTAACAGG	TCCAAGTGTTCTCCAAACCTT	55	239
	Exon 3	TCCATGCATTTTCCACAATC	TCTATTTTGGCAGCGAGGTT	57	282
	Exon 4	CTGATAGCTGGACAGCCAAC	TTAAGGAAGGCAGACTTCTTAGC	57	308
	Exon 5	AATGGGGGATGGGGTAAG	TGGCATGCATGAATCTTACC	62	229
	Exon 6	TGTGACCCAGGGACACTAGC	AAGCCTCTCTTTTTTGGTGC	55	223
	Exon 7	AAGCCTCTCTTTTTTGGTGC	ATCAATGGGCCGTGACAC	57	234
	Exon 8	CCCACTCTGGAGCACTGTC	GGTGGTTCCAGCCAATGA	59	350
	Exon 9	GGGTGGATGGGAGATAACTACT	GAATGAAGTAGAAGAGAAGTGAAGG	57	256
	Exon 10	AAGGGAAACTCTAATTATAGACCTTG	AATTCTTTCCAAATGGCTATAGGG	55	243
	Exon 11	TGGTTTTCAGCCTCCTCATA	GCATTGCAAAGAAAAGAATCAAA	55	428
hOCT3	5'-UTR	GCGCAGGAGGCCTCCGCACGCGCAA	GCGAAGGTGACGCCCGTCAGGCACA	68	673
	5'-UTR	CAATAAGTAAGCGGAAAAACCAGG	GCAGTCAGCCCCAGGTCG	68	537
	5'-UTR	GGACCGAGAGACAGGAGGGC	GGCTTGCTCAGCGTCCAGG	68	679
	5'-UTR	TGGAGACAAAGCAGGAAAGGG	CTCTTAGGTCATCTCGGCTTGG	58	656
	5'-UTR	GTCCACAGGGAACAATTTGAGG	GCCATCTGCCTCTTGTCAGTG	58	599
	Exon 1	AGGCCGCCGGCTGGGTCCGCGGGTC	CGACCTCCCCTGGCGGCCAGCGTCTC	68	594
	Exon 2	AAGATAAGGTGTTTTGAAGATCTGC	ATAAAACATTTTTCTCCCCGTATTA	58	243
	Exon 3	ATGTTATATTTTCCCATTGTGTTGA	ATAAAACATTTTTCTCCCCGTATTA	61	279
	Exon 4	TGTATTTGTTTGTTTATTTTGGAGC	ATTTTCATGTCTGTTTGGAGTCTAA	58	309
	Exon 5	TCAAGGCAATAGATTTTAGCGTT	CAAGAAGCAACAAAATCAATTCAC	58	250
	Exon 6, 7	TCTGTCTATTGCTACTGAAATCTGC	GGCTCCCTATACTTGATTGTGG	55	545
	Exon 8	TAAAATGTTAATGAAATCAGACCCC	GGCTCCCTATACTTGATTGTGG	58	237
	Exon 9	GTTGATTATCTTGAAGTCACTTGTTG	GTACAAAGAATGTAGATGAAGGCTC	58	227
	Exon 10	GAGAGCCCAGCTGTGTCTTC	TTCTTTCCCCCGTGGTTT	61	215
	Exon 11	CAGAACACCCTCTTCTAACTAGTTAC	CTTTGCAAGGAGGATCAGC	61	182
For Pyrosequencing primers					
hOCT1	P283L	ACGTCAGACCGAGGAAAATG	Biotin-CAGACGAATCTGCACCAGAA	64	229
		(seqencing : 5'- TGA ACA CGG TGG TGA –3')			
	P341L	Biotin-GCTCATGACAGCGTGAGTGT	CCCCTCACCACAGGTACATC	64	160
		(seqencing : 5'- TGCGCTTCCTCAGGC –3')			
hOCT2	T199I, T201M	TTTTCTTCCTGCAGGTTTGG	Biotin-TCTATTTTGGCAGCGAGGTT	58	228
		(seqencing : 5'- GGCCATTTCCCCAA –3')			
	A270S	ATACAGTTGGGCTCCTGGTG	Biotin-GGGTCTGGAGAGTGAAAGCA	64	227
		(seqencing : 5'- GGTTGCAGTTCACAGT –3')			

TABLE 2. Summary of genetic variations identified from *hOCT1*, *hOCT2*, and *hOCT3* genes in Korean subjects [b]

Genes	SNPs	Positions	Type of change	Amino acid	Functional consequences	Nucleotide Change and flanking sequences (5' to 3')	Allele frequency (%)
hOCT1	-1795 G>A	5'-UTR	-	-	ND	TGCCAAATGGCCA[**G/A**]TTGAATTCATGGAG	59
	-1714 G>A [a]	5'-UTR	-	-	ND	GAGAGAAACCAAAA[**G/A**]TCTGACTGGTAAG	2
	-1678 T>A [a]	5'-UTR	-	-	ND	ACCCTTTCGCCAGCA[**T/A**]GTCAGGCTGCTGA	2
	-206 G>A [a]	5'-UTR	-	-	ND	AAACGATTTGATCA[**G/A**]ATGGCCACGTGCA	9
	-129 G>A [a]	5'-UTR	-	-	ND	TTGGTTGCCTTCCA[**G/A**]ATGTTTCACACTTG	13
	156 T>C	Exon 1	Synonymous	S52S	ND	CACCACTGCCAGAG[**T/C**]CCTGGGGTGGCTG	35
	480 C>G	Exon 2	Nonsynonymous	**F160L**	No change [c,d]	AATGCGGGCTTCTT[**C/G**]TTTGGCTCTCTCGG	13
	848 C>T	Exon 5	Nonsynonymous	**P283L**	Decrease [e]	CTACTGGTGTGTGC[**C/T**]GGAGTCCCCTCGG	2
	E5+45 G>A [a]	Intron	Noncoding	-	ND	CTGAATCTGGGGCT[**G/A**]GGTTCTGGTGCAG	18
	1022 C>T	Exon 6	Nonsynonymous	**P341L**	Decrease [e]	CCTGTTCCGCACGC[**C/T**]GCGCCTGAGGAAG	16
	1222 A>G	Exon 7	Nonsynonymous	**M408V**	No change [c,d]	TCTACCCCATGGCC[**A/G**]TGTCAAATTTGTTG	74
hOCT2	-1733 A>G [a]	5'-UTR	-	-	ND	CGCAGTGGAGGTCA[**A/G**]TGGATGTCCTTGC	1
	-1629 A>G [a]	5'-UTR	-	-	ND	CTCCTTTTAGACTAC[**A/G**]CTATTACACCTGC	1
	-1604 T>C [a]	5'-UTR	-	-	ND	TGCTGACTATCCAA[**T/C**]AGAAAAAAGAAGG	7
	-1525 A>G [a]	5'-UTR	-	-	ND	AGGCCACCTTCTCT[**A/G**]CTTGGCAGGATCAC	48
	390 G>T	Exon 1	Synonymous	T130T	ND	TGGGTGTACGAGAC[**G/T**]CCTGGCTCGTCCA	15
	E2+32 C>G	Intron	Noncoding	-	ND	TGGTGGAATTTAAA[**C/G**]AATCCCAAAGGTTT	87
	596 C>T	Exon 3	Nonsynonymous	**T199I**	Decrease [f]	TGCCATTTCCCCAA[**C/T**]CTATACGTGGATGT	1
	602 C>T	Exon 3	Nonsynonymous	**T201M**	Decrease [f]	TTTCCCCAACCTATA[**C/T**]GTGGATGTTAATT	2
	808 G>T	Exon 4	Nonsynonymous	**A270S**	Decrease [f,g,h]	TGCAGTTCACAGTT[**G/T**]CTCTGCCCAACTTC	14
	1506 G>A	Exon 10	Synonymous	V502V	ND	TTTGGCTTTCAGGC[**G/A**]TGCTTGGCTTGGTT	85
hOCT3	-2269 C>T [a]	5'-UTR	-	-	ND	AACCCTGAGGGGAG[**C/T**]CCAAGGCAATCAC	27
	-1603 G>A [a]	5'-UTR	-	-	ND	TTCTGGGTAAGGG[**G/A**]CAGGTTCTTCTGTGG	25
	-1547 T>G [a]	5'-UTR	-	-	ND	CAAGGTAGAACAG[**T/G**]TGATTTCTTTATGGC	25
	-29 A>G	5'-UTR	-	-	ND	ACTCCGAGGCGCG[**A/G**]GCTGCGGGCGGCGG	68
	360 T>C	Exon 1	Synonymous	R120R	ND	CCTTCCCCAACCG[**T/C**]TCGGCTCCCCTTGTG	73
	579 C>T [a]	Exon 3	Synonymous	G193G	ND	GCCTTGGTGTTGG[**C/T**]GTCACTGGGGTTGTG	2
	E5+18 T>A [a]	Intron	Noncoding	-	ND	GAGGTAATTTCTT[**T/A**]CAGTATGAGTAACAA	1
	1233 G>A	Exon 7	Synonymous	A411A	ND	CGCCTCCCCTTTGC[**G/A**]GCAAGCAATATAGT	50

[a]**:** Novel mutations detected in this study.

[b]: For nucleotide numbering the A of the translation initiation codon ATG is denoted +1.

[c]: Kerb et al.,2002 ; [d]: Shu et al.,2003; [e]: Sakata et al., 2004

[f]: this study ; [g]: Fujita et al., 2006 ; [h]: Leabman et al., 2002

ND: Not determined

TABLE 3. Allele frequencies of *hOCT1* and *hOCT2* genetic variants in 4 different ethnic subjects

Polymorphisms		Ethnicity	N	Genotype			Allele frequency (%) (95% CI)	
				CC	**CT**	**TT**	**C**	**T**
hOCT1	P283L (848 C>T)	Korean	150	146	4	0	98.7 (97.7, 99.6)	1.3 (0, 3.2)
		Vietnamese	100	100	0	0	100	0
		Chinese	100	99	1	0	99.5 (98.8, 100)	0.5 (0, 1.9)
		German Caucasian	100	100	0	0	100	0
				CC	**CT**	**TT**	**C**	**T**
	P341L (1022 C>T)	Korean	150	101	48	1	83.3 (80.8, 85.9)	16.7 (10.7, 22.6)
		Vietnamese	100	89	11	0	94.5 (92.3, 96.7)	5.5 (1.0, 10.0)
		Chinese	100	79	20	1	89.0 (86.2, 91.8)	11.0 (4.9, 17.1)
		German Caucasian	100	96	4	0	98.0 (96.6, 99.4)	2.0 (0, 4.7)*
hOCT2				**CC**	**CT**	**TT**	**C**	**T**
	T199I (596 C>T)	Korean	150	148	2	0	99.3 (98.7, 100)	0.7 (0, 2.0)
		Vietnamese	100	100	0	0	100	0
		Chinese	100	100	0	0	100	0
		German Caucasian	100	100	0	0	100	0
				CC	**CT**	**TT**	**C**	**T**
	T201M (602 C>T)	Korean	150	148	2	0	99.3 (98.7, 100)	0.7 (0, 2.0)
		Vietnamese	100	97	3	0	98.5 (97.3, 99.7)	1.5 (0, 3.9)
		Chinese	100	100	0	0	100	0
		German Caucasian	100	100	0	0	100	0
				GG	**GT**	**TT**	**G**	**T**
	A270S (808 G>T)	Korean	150	118	31	1	89.0 (86.7, 91.3)	11.0 (6.0, 16.0)
		Vietnamese	100	73	27	0	86.5 (83.5, 89.5)	13.5 (6.8, 20.2)
		Chinese	100	75	22	3	86.0 (83.0, 89.0)	14.0 (7.2, 20.8)
		German Caucasian	100	95	5	0	97.5 (96.0, 99.0)	2.5 (0, 5.6)*

N: number of subjects.

95% CI: 95% confidence intervals.

*: $p < 0.05$, according to the χ^2 test.

Figure 1

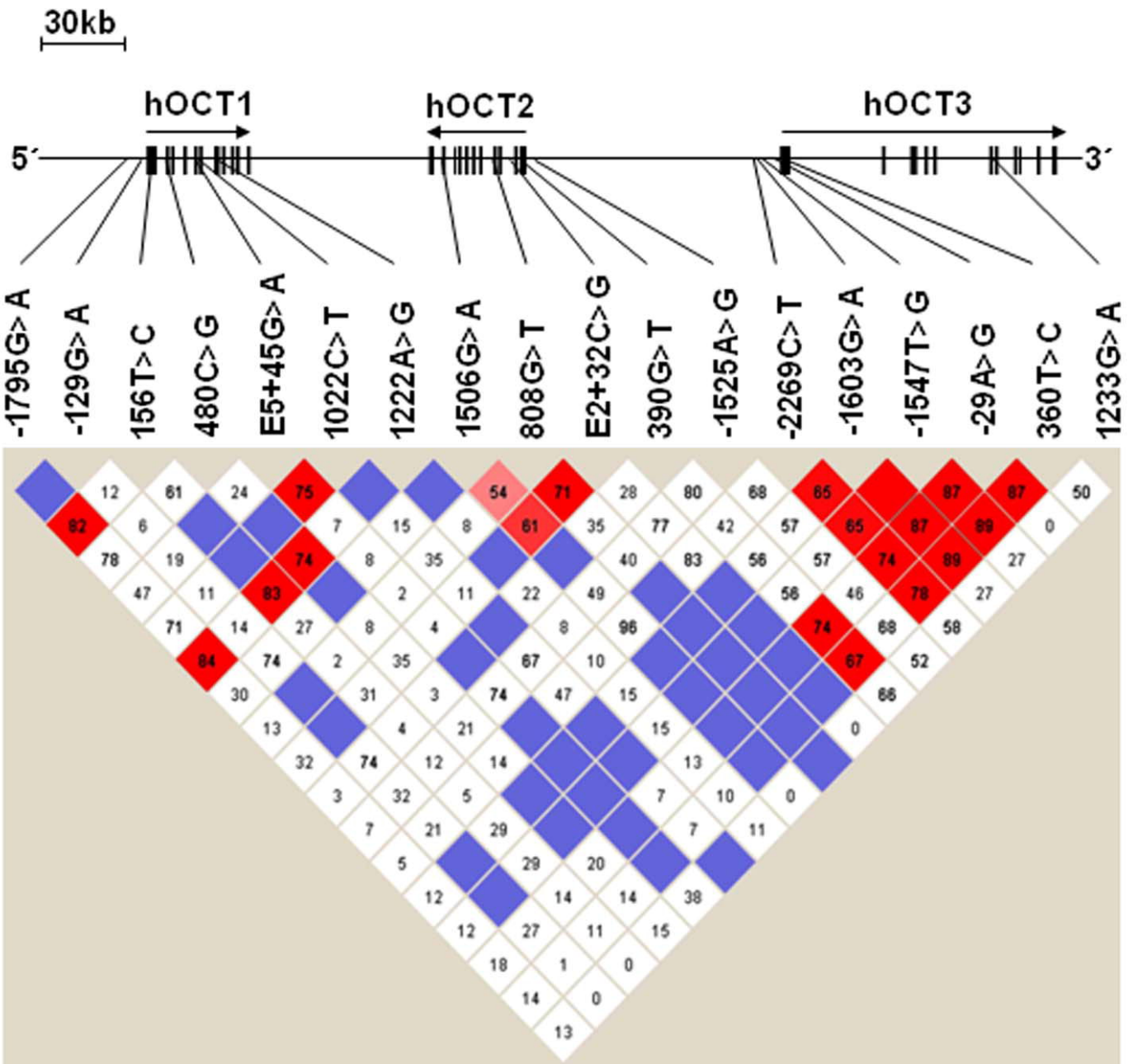
30kb
hOCT1
hOCT2
hOCT3
5´
3´
-1795G> A
-129G> A
156T> C
480C> G
E5+45G> A
1022C> T
1222A> G
1506G> A
808G> T
E2+32C> G
390G> T
-1525A> G
-2269C> T
-1603G> A
-1547T> G
-29A> G
360T> C
1233G> A

Figure 2

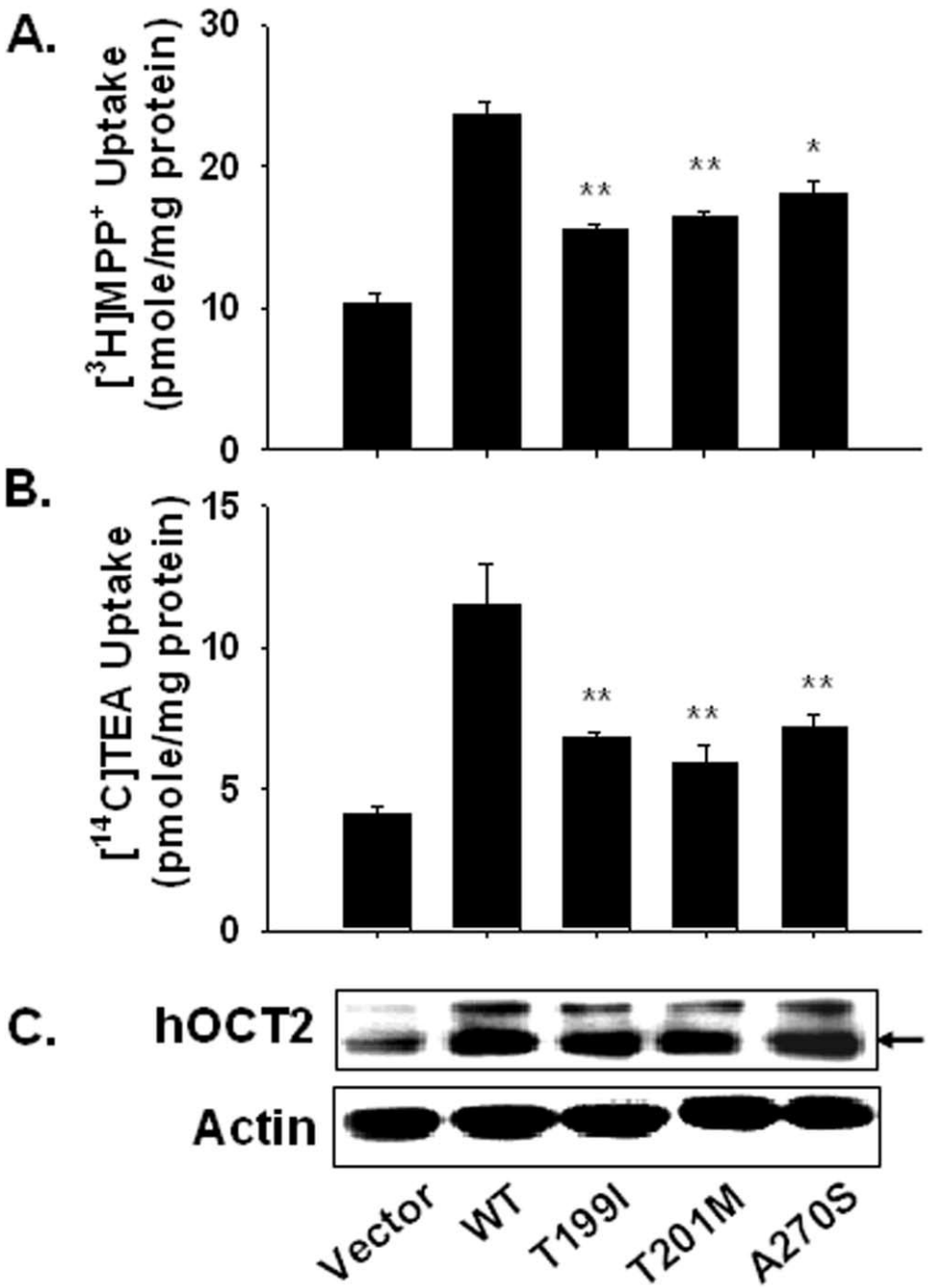
A.
[3H]MPP+ Uptake
(pmole/mg protein)
30
20
10
0
**
**
*
B.
[14C]TEA Uptake
(pmole/mg protein)
15
10
5
0
**
**
**
C.
hOCT2
Actin
Vector
WT
T199I
T201M
A270S

Figure 3

A. Concentration Dependency

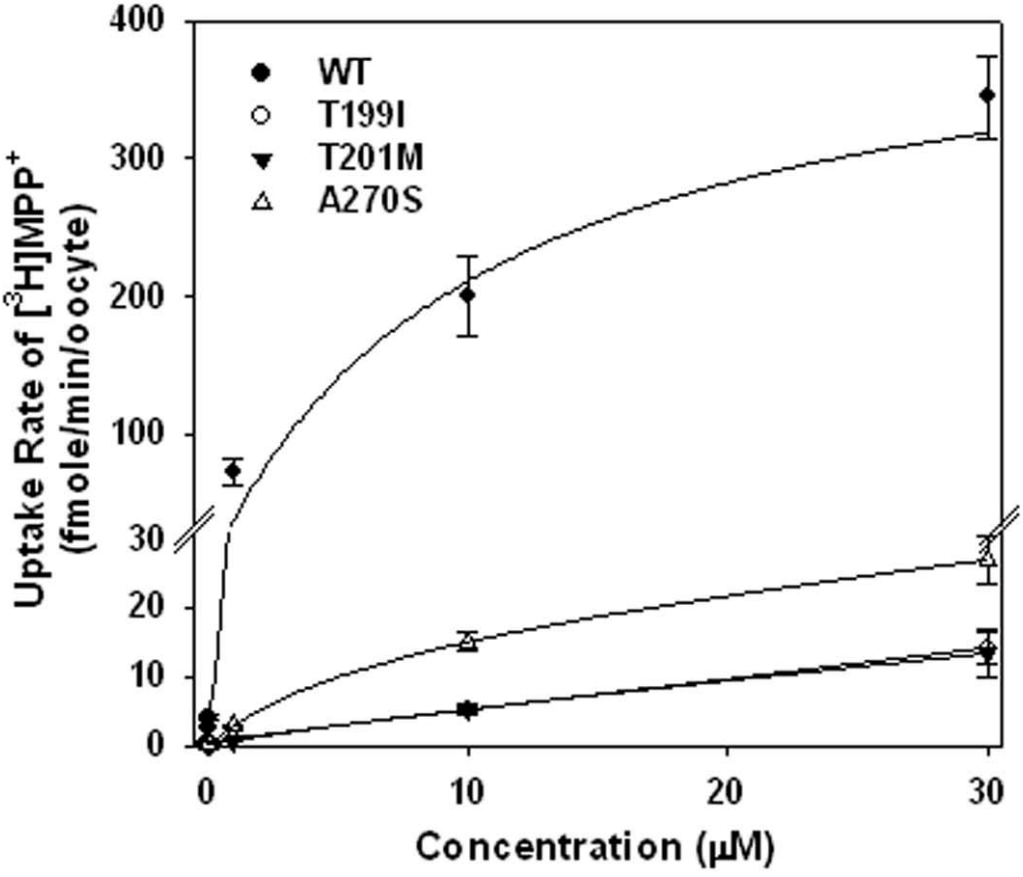

B. Kinetic Parameters

	V_{max} (fmole/min/oocyte)	K_m (μM)	CL_{int} (nL/min/oocyte)
WT	316.8	3.48	91.03
T199I	14.1	12.96	1.09
T201M	14.6	17.70	0.82
A270S	27.1	6.98	3.88

Figure 4

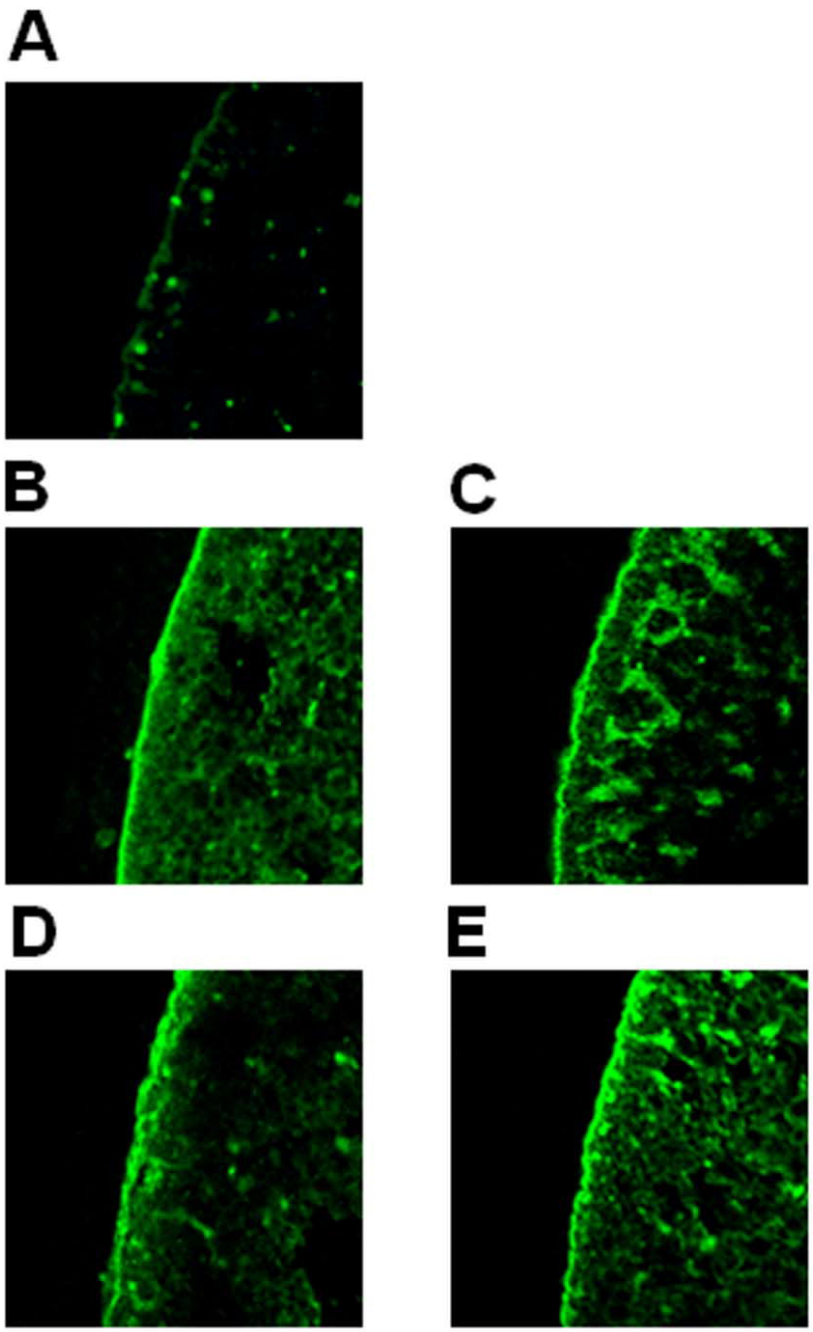

Figure 5

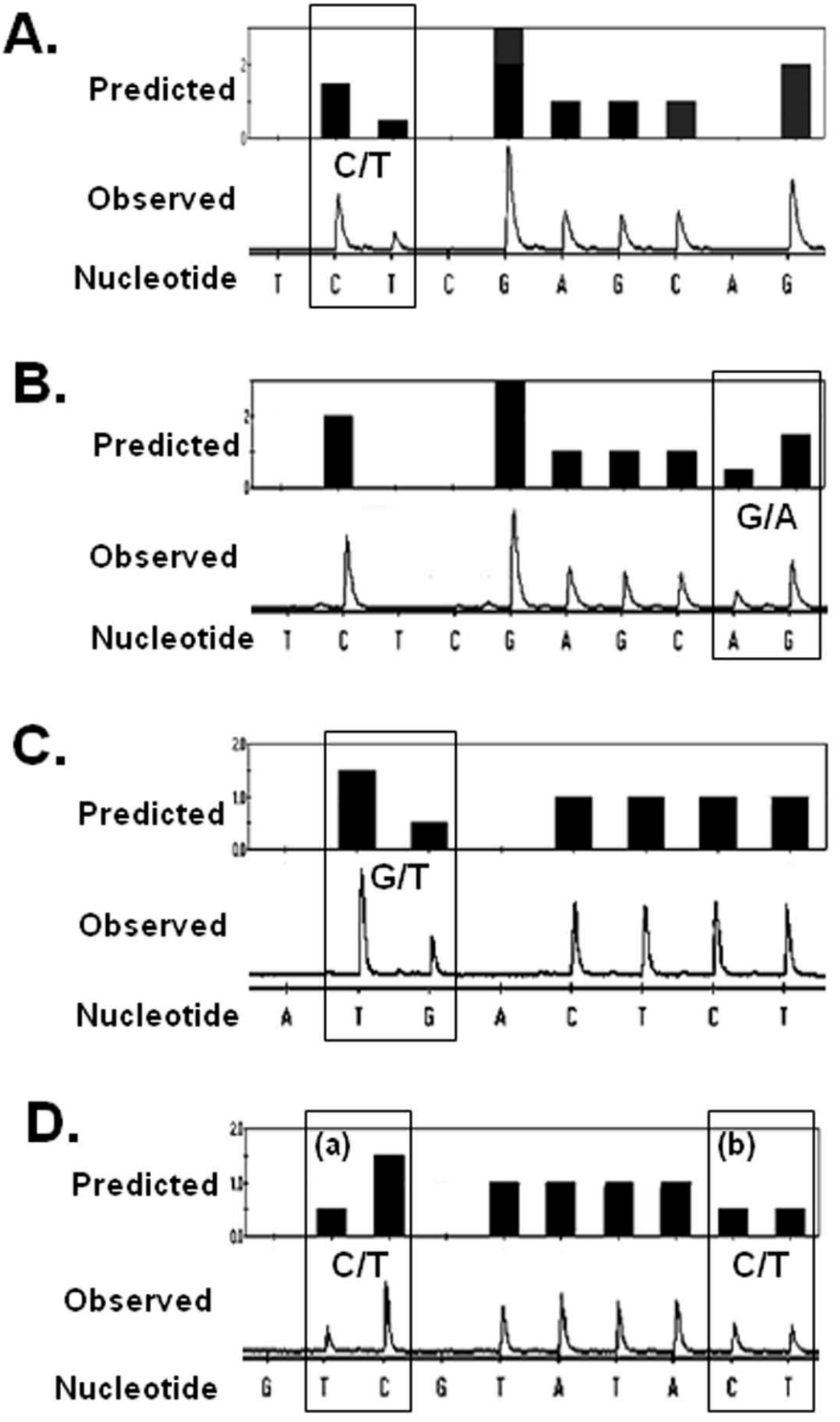
A.
Predicted
C/T
Observed
Nucleotide
T C T C G A G C A G
B.
Predicted
G/A
Observed
Nucleotide
T C T C G A G C A G
C.
Predicted
G/T
Observed
Nucleotide
A T G A C T C T
D.
(a)
(b)
Predicted
C/T
C/T
Observed
Nucleotide
G T C G T A T A C T